ISSN 1674-1056
http://cpb.iphy.ac.cn
http://iopscience.iop.org/cpb
中国物理 B
Chinese Physics
中国物理 Chinese Physics B

Triphenylene adsorption on Cu(111) and relevant graphene self-assembly

Qiao-Yue Chen(陈乔悦)[1], Jun-Jie Song(宋俊杰)[3], Liwei Jing(井立威)[1], Kaikai Huang(黄凯凯)[1], Pimo He(何丕模)[1,2], Hanjie Zhang(张寒洁)[1]
Citation: Chin. Phys. B . 2020, 29(2): 026801 . **doi:** 10.1088/1674-1056/ab6583
Journal homepage: http://cpb.iphy.ac.cn; http://iopscience.iop.org/cpb

What follows is a list of articles you may be interested in

Interaction of two symmetric monovacancy defects in graphene

Wen-Yan Xu(徐文焱), Li-Zhi Zhang(张礼智), Li Huang(黄立), Yan-De Que(阙炎德), Ye-Liang Wang(王业亮), Xiao Lin(林晓), Shi-Xuan Du(杜世萱)
Chin. Phys. B . 2019, 28(4): 046801 . **doi:** 10.1088/1674-1056/28/4/046801

Adsorption and diffusion of F_2 molecules on pristine graphene

Yong Yang(杨勇), Fu-Chi Liu(刘富池), Yoshiyuki Kawazoe(川添良幸)
Chin. Phys. B . 2018, 27(10): 106801 . **doi:** 10.1088/1674-1056/27/10/106801

Charge distribution in graphene from quantum calculation

Ze-Fen Liang(梁泽芬), Sheng-Ling Ma(马生凌), Hong-Tao Xue(薛红涛), Fan Ding(樊丁), Jingbo Louise Liu, Fu-Ling Tang(汤富领)
Chin. Phys. B . 2018, 27(1): 016801 . **doi:** 10.1088/1674-1056/27/1/016801

Improvement of sensitivity of graphene photodetectorby creating bandgap structure

Ni-Zhen Zhang(张倪侦), Meng-Ke He(何孟珂), Peng Yu(余鹏), Da-Hua Zhou(周大华)
Chin. Phys. B . 2017, 26(11): 116803 . **doi:** 10.1088/1674-1056/26/11/116803

Direct measurements of conductivity and mobility in millimeter-sized single-crystalline graphene via van der Pauw geometry

Rui-Song Ma(马瑞松), Qing Huan(郇庆), Liang-Mei Wu(吴良妹), Jia-Hao Yan(严佳浩), Yu-Yang Zhang(张余洋), Li-Hong Bao(鲍丽宏), Yun-Qi Liu(刘云圻), Shi-Xuan Du(杜世萱), Hong-Jun Gao(高鸿钧)
Chin. Phys. B . 2017, 26(6): 066801 . **doi:** 10.1088/1674-1056/26/6/066801

Triphenylene adsorption on Cu(111) and relevant graphene self-assembly*

Qiao-Yue Chen(陈乔悦)[1], Jun-Jie Song(宋俊杰)[3], Liwei Jing(井立威)[1], Kaikai Huang(黄凯凯)[1], Pimo He(何丕模)[1,2,‡], and Hanjie Zhang(张寒洁)[1,†]

[1] *Zhejiang Province Key Laboratory of Quantum Technology and Device, Department of Physics, Zhejiang University, Hangzhou* 310027, *China*
[2] *Collaborative Innovation Center of Advanced Microstructure, Nanjing University, Nanjing* 210093, *China*
[3] *Department of Fundamental and Social Science, Zhejiang University of Water Resources and Electric Power, Hangzhou* 310018, *China*

(Received 4 November 2019; revised manuscript received 16 December 2019; accepted manuscript online 25 December 2019)

Investigations on adsorption behavior of triphenylene (TP) and subsequent graphene self-assembly on Cu(111) were carried out mainly by using scanning tunneling microscopy (STM). At monolayer coverage, TP molecules formed a long-range ordered adsorption structure on Cu(111) with an uniform orientation. Graphene self-assembly on the Cu(111) substrate with TP molecules as precursor was achieved by annealing the sample, and a large-scale graphene overlayer was successfully captured after the sample annealing up to 1000 K. Three different Moiré patterns generated from relative rotational disorders between the graphene overlayer and the Cu(111) substrate were observed, one with 4° rotation between the graphene overlayer and the Cu(111) substrate with a periodicity of 2.93 nm, another with 7° rotation and 2.15 nm of the size of the Moiré supercell, and the third with 10° rotation with a periodicity of 1.35 nm.

Keywords: triphenylene, graphene, Cu(111), scanning tunneling microscopy

PACS: 68.43.Fg, 68.37.Ef, 68.43.–h **DOI:** 10.1088/1674-1056/ab6583

1. Introduction

Graphene has far-ranging prospects in many fields, such as materials, energy, optics, and electricity, due to its excellent performance and far-reaching potential application values. The precondition of graphene application is to fabricate high quality, large scale continuous graphene. Graphene was firstly obtained by mechanical exfoliation from the highly oriented pyrolytic graphite.[1] Since then, various methods for preparing graphene have been developed, including chemical exfoliation of graphite,[2] epitaxial growth on SiC under ultra-high vacuum and high temperature,[3] chemical vapor deposition (CVD),[4,5] and molecular self-assembly of graphene.[6] The present researches upon molecular self-assembly to grow graphene mainly use aromatic hydrocarbon molecules as the precursor molecules and then perform annealing operation on the surface of transition metals. This process is easy to operate and graphene grown by this method has advantages of high quality. Furthermore, the width and edge geometry of graphene nanoribbons can be controlled by adjusting the annealing temperature and the coverage range of the precursor molecules.[7,8] For example, the width and edge shape of synthesized graphene nanoribbons on the Au(111) surface can be precisely controlled by molecular self-assembly method;[9] using C60 as the precursor molecule, uniform size graphene quantum dots can be grown on the Ru(0001) surface through this method.[10,11] However, for different substrates and precursor molecules, conditions for growing graphene are quite different, and there are few related public studies at present.[9,12,13]

Copper is one of the most commonly used substrate for synthesizing graphene. The principle of growing graphene on Cu substrate is very different from that on other substrates because the solubility of carbon in copper is very low, therefore, the movement of carbon rings on the copper surface can be simply considered as surface-based motion.[14–16] Graphene can be synthesized on the copper substrates with various crystal orientations, but the Cu(111) substrate is most widely used as it is easier to grow high-quality single-layer graphene. The interaction between graphene and the Cu(111) substrate is weak,[17,18] so different Moiré patterns generated from relative rotational disorders between graphene and the Cu(111) substrate can be observed. At present, researchers have mainly observed two different superstructures: the Moiré pattern of 0° rotation of the graphene lattice with the underlying Cu(111) substrate (∼ 6.6 nm periodicity),[16,19,20] and the Moiré pattern of 7° rotation of the graphene lattice with the underlying Cu(111) substrate (∼ 2 nm periodicity).[20–22] The Moiré pattern of 10.4° misorientation has also been found in recent experiments.[23]

In this paper, we chose triphenylene ($C_{18}H_{12}$, TP) as the precursor molecule to investigate the graphene self-assembly on the Cu(111) surface and analyzed Moiré patterns which

*Project supported by the National Key Research and Development Program of China (Grant No. 2017YFB0503100) and the National Natural Science Foundation of China (Grant No. 11790313).

†Corresponding author. E-mail: zhj_fox@zju.edu.cn
‡Corresponding author. E-mail: phypmhe@zju.edu.cn

© 2020 Chinese Physical Society and IOP Publishing Ltd

formed with different misorientation angles. With scanning tunneling microscopy (STM), we first studied the growth and adsorption behavior of TP molecules on Cu(111) and then the processing of transforming TP molecules to graphene in the case of monolayer coverage. Finally, we analyzed the superstructures of different misorientation angles formed by aligning the graphene overlayer to the Cu(111) substrate rotationally.

2. Experimental and computational section

All the experiments were carried out in the ultra-high-vacuum variable temperature scanning probe system of Omicron, and the base pressure was better than 2×10^{-10} mbar. The system is consisted of a fast-entry lock, a sample preparation chamber, a sample analysis chamber, and an STM chamber.[24] The Cu(111) surface was cleaned by multiple cycles of argon ion sputtering (1000 eV for 1 hour) and subsequent high temperature annealing (at about 800 K). The cleanness and ordering of the sample were checked by low energy electron diffraction (LEED) and STM. Prior to experiment, TP was thoroughly degassed in a molecular beam epitaxy (MBE) chamber in a self-made tantalum boat. Before sublimation, the source was preheated under the heating power of 0.15 W. At the same time, the Cu(111) substrate remained unchanged at RT. During sublimation, the heating power was increased to 0.28 W, and maintained for 3 min. After 3 min of heating, the sample was directly opposed to the source for 10 s, and the growth rate of the film was about 0.1 ML/s. Afterwards the sample was directly passed to the analysis chamber for measurement. The pressure in the chamber was about 2×10^{-9} mbar during the film growth. STM measurements were conducted using constant current mode at RT. All the bias voltages were applied to the sample with respect to the tip. All experimental STM images in this paper were processed by WSxM software.[25]

3. Results and discussion

3.1. Adsorption of TP molecules on the Cu(111) surface

At sub-monolayer coverage, single TP molecule can not be imaged by STM at room temperature because of its high molecular mobility. This manifests the weak interaction between TP and Cu(111). For example, in order to visualize a single benzene ring on Cu(111) under low-coverage, both STM tip and substrate need to be putted in low temperature ($\sim$ 5 K) during the experiment and when the temperature arrives at 77 K, the benzene ring starts to diffuse freely.[16,19,26,27] It has also shown that the interaction between aromatic hydrocarbon molecules and the Cu (111) substrate is always weak.[4–6,28–30] After $\sim$ 1 ML of TP deposition, the structure of TP molecules on Cu (111) substrate was successfully resolved at RT. Anyway, the adsorption energy of single TP molecule is higher than that of a benzene ring,[31] and a two-dimensional closely packed adsorption layer certainly enhanced the interaction between the molecules and substrate which minimized the influence of the tip–molecule interaction and the temperature. Previous investigations have already proven that planar TP molecules show a stable flat-lying orientation at a wide range of bias voltages from -0.5 V to -0.01 V.[32] Indeed, the increased bias voltage and tunneling current excite locally the molecules by a moderate electric field and tip–surface interaction.[33] Actually, in the present STM measurements, the absolute bias voltages below 0.6 V were applied to avoid destroying the formed monolayer ordering.

At monolayer coverage, TP molecules formed a long-range ordered adsorption structure on the Cu(111) surface with uniform orientation, which is detailedly figured out in Fig. 1. Figure 1(a) shows a hexagonally close-packed domain formed by TP molecules, and molecular lines are along the [110] direction of the substrate. In the high resolution STM image of Fig. 1(b), the overall triangular shape and the benzene ring of a single molecule can also be seen faintly, and the unit cell of the flat-lying adsorption overlayer is outlined by the brown rhombus whose lateral size can be precisely determined with STM images. Figure 1(c) shows the line profile along the brown straight line outlined in Fig. 1(b), which elucidates the lateral average distance between the TP molecules.[16] Figure 1(d) illustrates the orientation of TP molecules with 3-fold symmetry and its lateral size of 1.23 nm.

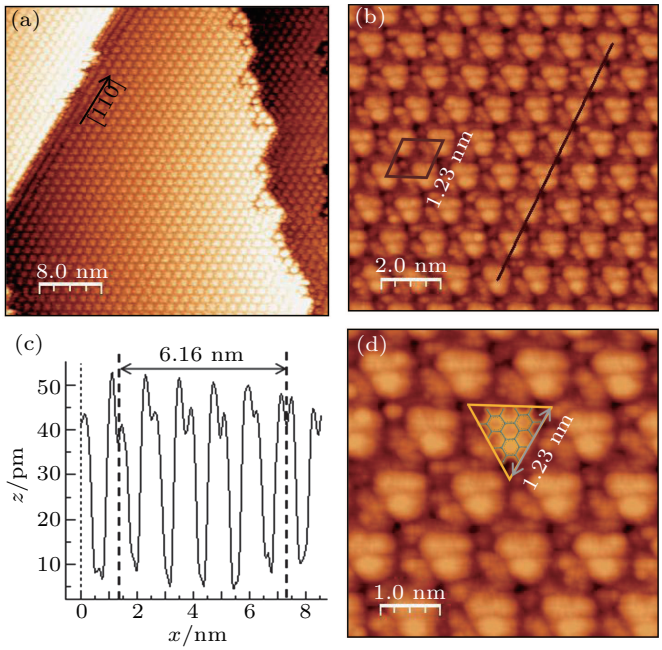


Fig. 1. (a) STM image with monolayer coverage of TP molecules on Cu(111) (50 nm×50 nm, $V_T = -0.516$ V, $I_T = 0.574$ nA). (b) High resolution STM image (10 nm×10 nm, $V_T = -0.447$ V, $I_T = 0.088$ nA). (c) Line profile along the straight line indicated in (b). (d) The enlarged STM image showing the molecular orientation in details.

In order to infer the specific adsorption sites of TP on the

Cu(111) surface, we first consider the possible adsorption sites of the single benzene ring on Cu(111) and its corresponding adsorption energy. Theoretical approach for benzene ring adsorption on Cu(111) shows that the three-fold hollow site is the most stable adsorption site (as shown in Fig. 2(a)), and the adsorption energy is 0.86 eV.[34,35] Therefore, we assume that the adsorption site of molecular self-assembly of TP on Cu(111) is also the hollow site which is shown in Fig. 2(b), and the supercell is p(5×5). Based on the theoretical calculation of the model, the molecule–molecule distance is 1.28 nm, which is consistent well with the experimental results. Besides, the interaction between TP and the Cu(111) surface is van der Waals one which is weak enough to manifest molecule–molecule weakly repulsive force. And in order to balance the repulsion between the molecules, they will finally choose hexagonally stacking order in the monolayer regime. The weak balance between the molecule–molecule repulsive and molecule–substrate attractive interactions favors 2D liquid-like growth which delicately forms a long-rang ordered superstructure.

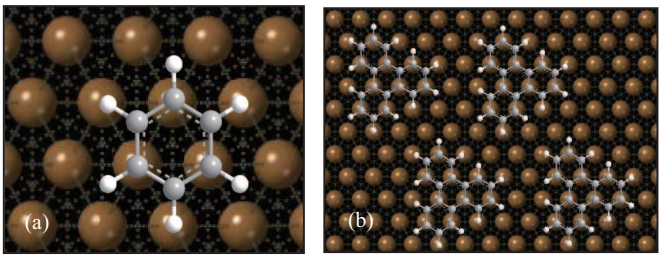


Fig. 2. (a) The ball and stick model for benzene at hollow site of Cu(111), where the brown, gray, and white balls represent copper, carbon, and hydrogen atoms, respectively. (b) The model structure for TP on Cu(111) surface with p(5×5) supersymmetry.

3.2. Graphene self-assembly on Cu(111) via TP molecules

In order to further investigate the conditions of graphene self-assembly on Cu(111) via TP molecules, the sample was first annealed at 600 K for 30 min. The catalytic influence of the substrate has been confirmed experimentally by the fact that cyclodehydrogenation on Cu(111) is already completed at 250 ℃.[36] Therefore, annealing at 600 K ensured the cyclodehydrogenation of the TP precursor on the Cu(111) surface. The afterwards STM measurements showed that only seldom graphene fragments whose sizes were smaller than 3 nm×3 nm were found at the step edges of the Cu(111) surface coexisting with products of polymerization (see Fig. S1 in supporting information). For TP molecules, without the stage of dehalogenation, the processes of polymerization and dehydrogenation destined to overlap on Cu(111) during which polymerization was easily stopped by the hydrogen passivation from forming C–H bonds.[36,37] Furthermore, the STM images collected for the sample under the annealing temperature of 700 K indicated that cyclodehydrogenation still moves on, and more graphene flakes have been synthesized (see Fig. S2). However, after further annealing at 800 K for 30 min (Fig. S3) or 900 K for 10 min (Fig. S4), both the number and lateral size of graphene islands almost showed no difference.

Finally, large-scale graphene films were successfully captured after sample annealing at 1000 K for 10 s, as shown in Fig. 3(a). Firstly, under the temperature of 1000 K, TP molecules dehydrogenate on the mental surface and form active surface species. Then these active species coalesce, nucleate, and grow to graphene.[38,39] Secondly, small-size graphene that has formed may dissociate to active species, and then coalesces into new graphene on Cu(111). Besides, rapid high-temperature annealing of the sample (at 1000–1100 K) gives rise to the removal of Cu oxide and the recovery of crystallographic features of the copper, which contribute to the interconnection among small-size graphene.[37,40] All the three reasons played important roles in forming large size graphene islands at 1000 K. Inferring from the STM images, grains of graphene always started from Cu(111) step edges. Moreover, the large size graphene islands invariably had boundaries as marked by the blow arrow in Fig. 3(a).[14] Different Moiré patterns generated from relative rotational disorders between graphene and the Cu(111) substrate have been observed. In the present case, three different Moiré patterns were mainly observed, which also suggested the preferable rotations of graphene aligning to the Cu(111) surface after 1000 K annealing. Until now, three types of rotational domains under aligning graphene to Cu(111) with periodicity of 1.35 nm, 2.15 nm, 2.95 nm have been observed. The STM image in Fig. 3(b) shows the Moiré pattern with periodicity of 2.15 nm which is the already known superstructure formed by 7° rotation misorientation between graphene and the Cu(111) substrate, we will not describe this pattern in details here.[20–22]

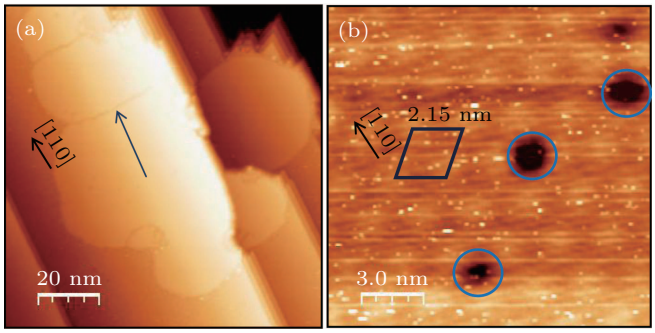


Fig. 3. (a) STM image of graphene self-assembly on Cu(111) substrate via TP molecules after 1000 K annealing (100 nm×100 nm, $V_T = -0.645$ V, $I_T = 0.661$ nA). The blue arrow refers to graphene boundaries. (b) Moiré pattern of graphene on Cu(111) at 7° misorientation angle (15 nm×15 nm, $V_T = -0.987$ V, $I_T = 0.282$ nA), and the blue circle in the figure indicates defects found on the surface. Both the black arrows indicate the [110] direction of Cu(111).

Based on the line profiles in STM images which are partly shown in Figs. 4(a) and 4(b), the height of the graphene overlayer is below 0.1 nm, which demonstrates that these islands are composed of single monolayer graphene. Hereinafter, we

discuss the other two Moiré patterns presented in the STM images. The reason for graphene forming superstructures on the Cu(111) surface is lattice mismatch, i.e., the lattice constants difference between graphene and the Cu(111) substrate (the lattice constants of graphene and Cu(111) are 0.246 nm and 0.256 nm, respectively).[41] Figure 4(c) shows the STM image of single-layer graphene on Cu (111) with a periodicity of 1.35 nm which is the smallest Moiré supercell. In the high resolution STM image of Fig. 4(d), the honeycomb structure of graphene can be clearly observed, and the average lateral size is determined to be about 0.235 nm, in comparison with the graphene lattice constant of 0.246 nm.

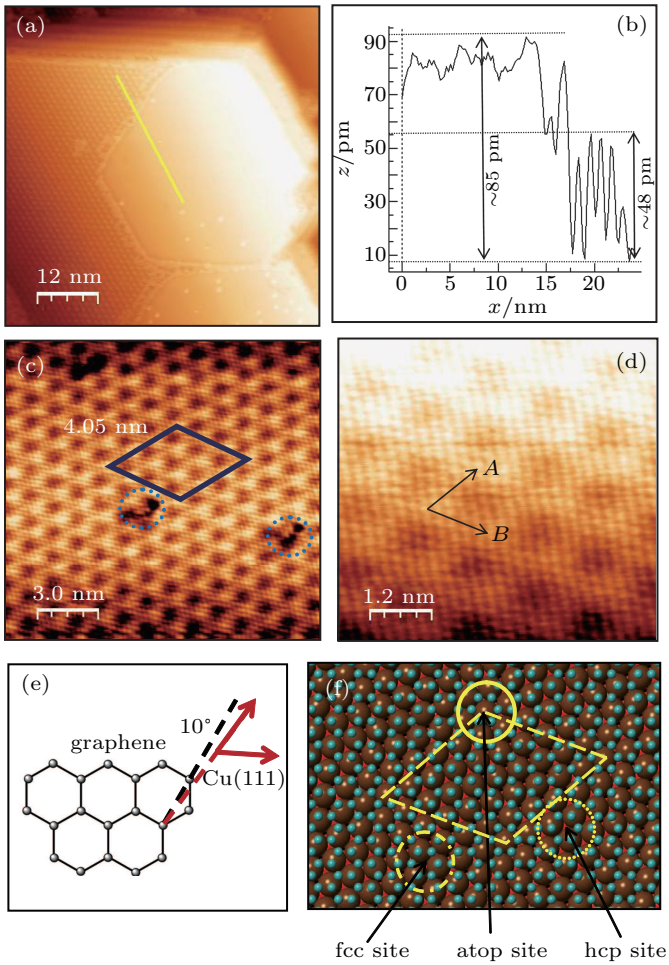


Fig. 4. (a) STM image of graphene coexistence with TP molecules (60 nm×60 nm, $V_T = -0.530$ V, $I_T = 0.972$ nA). (b) Line profile along the yellow straight line outlined in Fig. 3(a), and the apparent height of graphene and TP is around 85 pm and 48 pm, respectivley. (c) STM image of graphene on Cu (111) with a periodicity of 1.35 nm (15 nm×15 nm, $V_T = -0.183$ V, $I_T = 0.403$ nA). (d) High resolution STM image (6 nm×6 nm, $V_T = -0.429$ V, $I_T = 0.032$ nA), and the supercell is indicated by the basic vectors $A = B = 1.35$ nm. (e) The definition of 10° misorientation angle between graphene and Cu(111). (f) Simulation result through simply align graphene to Cu(111) with 10° rotation and the superscell is $(2\sqrt{7} \times 2\sqrt{7})$R20.3°, as outlined with yellow rhombus. The blue balls represent carbons and brown, red, black balls represent the first, second, third layer copper atoms. The fcc, hcp, and atop adsorption sites have been marked with yellow circles to describe the location of carbon rings on Cu(111).

Density functional theory (DFT) and classical molecular dynamics simulations (CMD) are the most commonly used theoretical methods for studying the behavior of graphene on metal surfaces.[23,36,42] Recent researches have shown that the interaction between graphene and the Cu(111) substrate is van der Waals force based on DFT calculations.[35,41,43,44] Süle *et al.* developed a new Albell–Tersolf-like angular-dependent potential for the C–Cu interaction, but the results of periodicity of patterns simulated through this method are somewhat a bit lager than the STM measurements. CMD simulation showed that the adsorption energy has a minimum value (a stable phase) at a rotational angle of 10.4° between graphene and Cu(111) with a Moiré periodicity of 1.4 nm,[23] which agrees well with the value of 1.35 nm determined based on the STM images. The simple simulation by superimposing graphene lattice (0.246 nm) on Cu(111) (0.256 nm) with a 10° rotational angle (Fig. 4(e)) is shown in Fig. 4(f). The simulated Moiré pattern is consistent with the STM topography and the supercell has a $(2\sqrt{7} \times 2\sqrt{7})$R20.3° symmetry which has been pointed out with yellow rhombus with a periodicity of 1.35 nm. The atop sites represent the regions where the center of the carbon hexagon is located on top of the copper atoms which is indicated by a yellow circle. The fcc site (dashed yellow circle) and hcp site (dotted yellow circle) are the threefold hollow sites where the center of the carbon hexagon is located on top of the second layer (red balls) or third layer (black balls) copper atoms. According to the binding of graphene to Ir(111) calculated by nonlocal van der Waals density functional approach, the topmost carbon atoms are those in the atop regions, and the lowest carbon atoms are those atoms located on the hcp site.[41,45–47] However, carbon atoms in the fcc and hcp regions have almost the same local adsorption configurations, so they almost show the same contrast in the STM images. Therefore, the atop sites are in accordance with the brightest domains while the hcp and fcc sites are in accordance with the darkest domains in the STM topographies (Figs. 4(c) and 4(d)). Actually, a neglectable corrugation in this Moiré pattern is determined to be around 0.05 nm with the STM images.

Figure 5(a) shows another Moiré pattern of the graphene lattice overlying on the Cu(111) substrate with a periodicity of 2.93 nm. In the higher resolution STM topography (Fig. 5(b)), the honeycomb structure of graphene can be observed legibly and the average lateral size is 0.235 nm. Figure 5(c) is the line profile along the blue straight line outlined in Fig. 5(b) from which we can derive the apparent height (0.07 nm) and the periodicity (3.05 nm) of the Moiré pattern. As Süle *et al.* predicted through CMD approach, there exists another stable phase at 2.2° rotation and the periodicity of the corresponding Moiré pattern is 4.3 nm, but it can not fit this situation. So we chose another CMD simulation taken the Lennard–Jones (L–J) potential as the van der Waals force between graphene and Cu(111) substrate which has inferred that the adsorption energy has a global minimum at the misorientation angle $\theta = 1°$

and local minima at $\theta = 3°, 6°, 8°, 10°$ with the measurement error of $\Delta\theta \approx 1°$.[34] Therefore, we simulated 4° rotational alignment of the graphene lattice with the underlying Cu(111) lattice and deduced the superstructure model of Fig. 5(d). This Moiré pattern, the supercell sketched as yellow rhombus in Fig. 4(d), has a $(\sqrt{133} \times \sqrt{133})$R4.3° supersymmetry with a periodicity of 2.95 nm, which is almost equal to the experimental value of 2.93 nm determined with STM images. Therefore, the superstructure of the periodicity of ~ 3 nm observed in this experiment is a Moiré pattern formed by the ~ 4° misorientation angle between graphene and Cu(111) surface. We can easily figure out the atop site (yellow circle), fcc site (dashed yellow circle), and hcp site (dotted yellow circle) in Fig. 5(d) as above. Although the theoretical calculation deduced that the atop site should be found in or close to the bright domains of the pattern, a contrast inversion was observed comparing the STM image with the simulation result.[35,45] Tunneling parameters and tip states play a significant function during photo acquisition, the tunneling voltage or the state of the tip both can induce such contrast inversion. All the blue dash circles indicated in the above pictures are defects found on the surface of graphene which may form to release the surface stress due to lattice mismatch.[16,48]

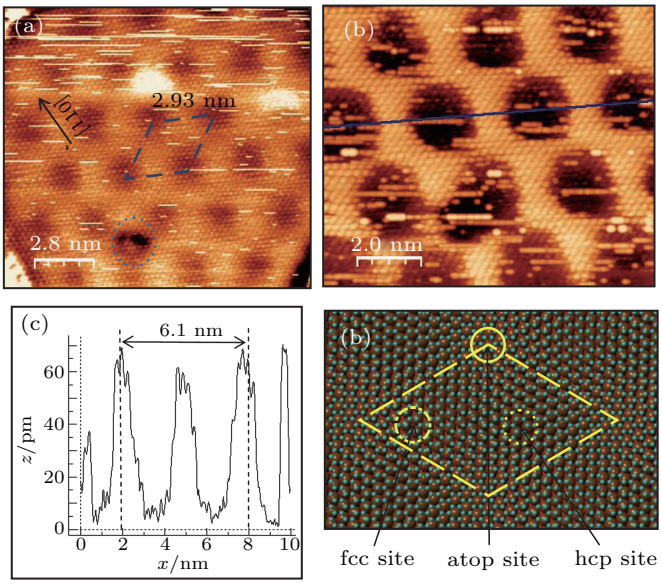


Fig. 5. (a) STM topography of superstructure of graphene on Cu (111) with a periodicity of 2.93 nm (14 nm×14 nm, $V_T = -0.172$ V, $I_T = 0.558$ nA), and the black arrow indicates the [110] direction of Cu(111). (b) High resolution STM topography (10 nm×10 nm, $V_T = -0.183$ V, $I_T = 0.403$ nA). (c) Line profile along the blue straight line outlined in Fig. 3(b). (d) Simulation result through simply align graphene to Cu(111) with 4° rotation and the superscell is $(\sqrt{133} \times \sqrt{133})$R4.3°, as outlined with yellow rhombus. The blue balls represent carbons and brown, red, black balls represent the first, second, third layer copper atoms. The fcc, hcp, and atop adsorption sites have been marked with yellow circles to describe the location of carbon rings on Cu(111).

4. Conclusions

In summary, we have investigated the growth of self-assembly graphene on the Cu(111) surface by using TP molecules as precursor and the Moiré patterns of graphene on Cu(111). At monolayer coverage, the weak balance between the molecule–molecule repulsive and molecule–substrate attractive interactions has favored 2D liquid-like growth which delicately formed a long-rang ordered superstructure. During sample annealing, at temperature ≤ 900 K, only small-scale graphene fragments can form. But after annealing at higher temperature (1000 K), the dissociation of TP molecules and small graphene dissociation, removal of Cu oxide, and increasing mobility of graphene islands contribute to forming the large-scale graphene. Three different Moiré patterns generated from relative rotational disorders between graphene and the Cu(111) substrate have been observed and according to the result inferred from DFT and CMD, we map each pattern to its corresponding rotation: one with 4° rotation between graphene lattice and the Cu(111) substrate with the periodicity of 2.93 nm which has not been found in other research, another with 7° rotation and the size of the Moiré supercell is 2.15 nm, and the third with 10° rotation with a periodicity of 1.35 nm.

References

[1] Novoselov K S, Geim A K, Morozov S V, Jiang D, Zhang Y, Dubonos S V, Grigorieva I V and Firsov A A 2004 *Science* **306** 666
[2] Blake P, Brimicombe P D, Nair R R, Booth T J, Jiang D, Schedin F, Ponomarenko L A, Morozov S V, Gleeson H F, Hill E W, Geim A K and Novoselov K S 2008 *Nano Lett.* **8** 1704
[3] Forbeaux I, Themlin J M and Debever J M 1998 *Phys. Rev.* **58** 16396
[4] Li X S, Cai W W, An J, Kim S, Nah J, Yang D X, Piner R, Velamakanni A, Jung I, Tutuc E, Banerjee S K, Colombo L and Ruoff R S 2009 *Science* **324** 1312
[5] Zhang X B, Qing F Z and Li X S 2019 *Acta Phys. Sin.* **68** 96801 (in Chinese)
[6] Li J, Gottardi S, Solianyk L, Moreno-López J C and Stöhr M 2016 *J. Phys. Chem. C* **120** 18093
[7] Song J J, Zhang Y X, Zhang H J, Cai Y L, Bao S N and He P M 2016 *Appl. Surf. Sci.* **367** 424
[8] Song J J, Zhang H J, Cai Y L, Zhang Y X, Bao S N and He P M 2015 *Nanotechnology* **27** 055602
[9] Cai J, Ruffieux P, Jaafar R, Bieri M, Braun T, Blankenburg S, Muoth M, Seitsonen A P, Saleh M, Feng X, Müllen K and Fasel R 2010 *Nature* **466** 470
[10] Lu J, Yeo P S E, Gan C K, Wu P and Loh K P 2011 *Nat. Nanotechnol.* **6** 247
[11] Zhu R J, Huang Y H, Li J Y, Kang N and Xu H Q 2019 *Chin. Phys. B* **28** 67201
[12] Fang W, Hsu A L, Song Y and Kong J 2015 *Nanoscale* **7** 20335
[13] Suzuki N, Wang Y, Elvati P, Qu Z B, Kim K, Jiang S, Baumeister E, Lee J, Yeom B, Bahng J H, Lee J, Violi A, Kotov N A, Michigan U and Ann Arbor M I 2016 *ACS Nano* **10** 1744
[14] Zhou Z, Gao F and Goodman D W 2010 *Surf. Sci.* **604** L31
[15] Didar B R, Khosravian H, Balbuena P B, *et al.* 2018 *RSC Adv.* **8** 27825
[16] Niu T C, Zhou M, Zhang J L, Feng Y P and Chen W 2013 *J. Am. Chem. Soc.* **135** 8409
[17] Batzill M 2012 *Surf. Sci. Rep.* **67** 83
[18] Xu Z and Buehler M J 2010 *J. Phys.: Condens. Matter* **22** 485301
[19] Soy E, Liang Z and Trenary M 2015 *J. Phys. Chem. C* **119** 24796
[20] Gao L, Guest J R and Guisinger N P 2010 *Nano Lett.* **10** 3512
[21] Nguyen V L, Shin B G, Duong D L, Kim S T, Perello D, Lim Y J, Yuan Q H, Ding F, Jeong H Y, Shin H S, Lee S M, Chae S H, Vu Q A, Lee S H and Lee Y H 2015 *Adv. Mater.* **27** 1376
[22] Chen X, Liu S Y, Liu L C, Liu X Q, Liu X M and Wang L 2012 *Appl. Phys. Lett.* **100** 163106
[23] Süle P, Szendrő M, Hwang C and Tapasztó L 2014 *Carbon* **77** 1082

[24] Lu B, Zhang H J, Li H Y, Bao S N, He P and Hao T L 2003 *Phys. Rev. B* **68** 125410
[25] Horcas I, Fernández R, Gómez-Rodríguez J M, Colchero J, Gómez-Herrero J and Baro A M 2007 *Rev. Sci. Instrum.* **78** 013705
[26] Tonigold K and Groß A 2010 *J. Chem. Phys.* **132** 224701
[27] Yan S C, Xie N, Gong H Q, Sun Q, Guo Y, Shan X Y and Lu X H 2012 *Chin. Phys. Lett.* **29** 46803
[28] Ge S P, Lu C and Zhao R G 2006 *Chin. Phys. Lett.* **23** 1558
[29] Qi J, Gao Y X, Huang L, Lin X, Dong J J, Du S X and Gao H J 2019 *Chin. Phys. B* **28** 66801
[30] Song Z P, Bao L, Cao Y, Qi J, Peng H, Wang Q, Huang L, Lu H L, Lin X, Wang Y L, Du S X and Gao J H 2019 *Chin. Phys. B* **28** 56801
[31] Zint S R, Ebeling D, Ahles S, Wegner H A and Schirmeisen A 2016 *J. Phys. Chem. C* **120** 1615
[32] Xu Q M, Han M J, Wan L J, Wang C, Bai C L, Dai B and Yang J L 2003 *Chem. Commun.* **9** 2874
[33] Krüger P, Petukhov M, Domenichini B, Berkó A and Bourgeois S 2012 *J. Phys. Chem. C* **116** 10617
[34] Bilić A, Reimers J R, Hush N S, Hoft R C and Ford M J 2006 *J. Chem. Theory Comput.* **2** 1093
[35] Liu W, Ruiz V G, Zhang G X, Santra B, Ren X, Scheffler M and Tkatchenko A 2013 *New J. Phys.* **15** 53046
[36] Talirz L, Ruffieux P and Fasel R 2016 *Adv. Mater.* **28** 6222
[37] Talirz L, Söde H, Cai J, Ruffieux P, Blankenburg S, Jafaar R, Berger R, Feng X, Müllen K, Passerone D, Fasel R and Pignedoli C A 2013 *J. Am. Chem. Soc.* **135** 2060
[38] Wan X, Chen K, Liu D Q, Chen J, Miao Q and Xu J B 2012 *Chem. Mater.* **24** 3906
[39] Chen K, Wan X, Liu D Q, Kang Z W, Xie W G, Chen J, Miao Q and Xu J B 2013 *Nanoscale* **5** 5784
[40] Cho J, Gao L, Tian J F, Cao H L, Wu W, Yu Q K, Yitamben E N, Fisher B, Guest J R, Chen Y P and Guisinger N P 2011 *ACS Nano* **5** 3607
[41] N'Diaye A T, Coraux J, Plasa T N, Busse C and Michely T 2008 *New J. Phys.* **10** 043033
[42] Zhao M W, Xia Y Y, Ma Y C, Ying M J, Liu X D and Mei L M 2002 *Chin. Phys. Lett.* **19** 1498
[43] Sidorenkov A V, Kolesnikov S V and Saletsky A M 2016 *Eur. Phys. J. B* **89** 1
[44] He R, Zhao L Y, Petrone N, Kim K S, Roth M, Hone J, Kim P, Pasupathy A and Pinczuk A 2012 *Nano Lett.* **12** 2408
[45] Hattab H, N'Diaye A T, Wall D, Jnawali G, Coraux J, Busse C, van Gastel R, Poelsema B, Michely T, Meyer zu Heringdorf F J and Horn-von Hoegen M 2011 *Appl. Phys. Lett.* **98** 141903
[46] Murata Y, Petrova V, Kappes B B, Ebnonnasir A, Petrov I, Xie Y H, Ciobanu C V and Kodambaka S 2010 *ACS Nano* **4** 6509
[47] Busse C, Lazić P, Djemour R, Coraux J, Gerber T, Atodiresei N, Caciuc V, Brako R, N'Diaye A T, Blügel S, Zegenhagen J and Michely T 2011 *Phys. Rev. Lett.* **107** 036101
[48] Xu W Y, Zhang L Z, Huang L, Que Y D, Wang Y L, Lin X and Du S X 2019 *Chin. Phys. B* **28** 46801